



# Preparation of magnetic indole-3-acetic acid imprinted polymer beads with 4-vinylpyridine and $\beta$ -cyclodextrin as binary monomer via microwave heating initiated polymerization and their application to trace analysis of auxins in plant tissues

Yi Zhang<sup>a</sup>, Yuanwen Li<sup>a</sup>, Yuling Hu<sup>a,\*</sup>, Gongke Li<sup>a,\*\*</sup>, Yueqin Chen<sup>b</sup>

<sup>a</sup> School of Chemistry and Chemical Engineering, Sun Yat-sen University, Guangzhou 510275, China

<sup>b</sup> Key Laboratory of Gene Engineering of the Ministry of Education, State Key Laboratory for Biocontrol, Sun Yat-Sen University, Guangzhou 510275, China

## ARTICLE INFO

### Article history:

Received 18 August 2010

Received in revised form

17 September 2010

Accepted 23 September 2010

Available online 1 October 2010

### Keywords:

Auxin

Indole-3-acetic acid

Molecularly imprinted polymer beads

Magnetic separation

$\beta$ -Cyclodextrin

Microwave heating

## ABSTRACT

Auxin is a crucial phytohormone for precise control of growth and development of plants. Due to its low concentration in plant tissues which are rich in interfering substances, the accurate determination of auxins remains a challenge. In this paper, a new strategy for isolation and enrichment of auxins from plant tissues was obtained by the magnetic molecularly imprinted polymer (mag-MIP) beads, which were prepared by microwave heating initiated suspension polymerization using indole-3-acetic acid (IAA) as template. In order to obtain higher selective recognition cavities, an enhanced imprinting method based on binary functional monomers, 4-vinylpyridine (4-VP) and  $\beta$ -cyclodextrin ( $\beta$ -CD), was adopted for IAA imprinting. The morphological and magnetic characteristics of the mag-MIP beads were characterized by scanning electron microscopy, Fourier-transform infrared spectroscopy and vibrating sample magnetometry. A majority of resultant beads were within the size range of 80–150  $\mu\text{m}$ . Porous surface morphology and good magnetic property were observed. Furthermore, the mag-MIP beads fabricated with 4-VP and  $\beta$ -CD as binary functional monomers exhibited improved recognition ability to IAA, as compared with the mag-MIP beads prepared with the individual monomer separately. Competitive rebinding experiment results revealed that the mag-MIP beads exhibited a higher specific recognition for the template than the non-imprinted polymer (mag-NIP) beads. An extraction method by mag-MIP beads coupled with high performance liquid chromatography (HPLC) was developed for determination of IAA and indole-3-butyric acid (IBA) in plant tissues. Linear ranges for IAA and IBA were in the range of 7.00–100.0  $\mu\text{g L}^{-1}$  and 10.0–100.0  $\mu\text{g L}^{-1}$ , and the detection limits were 3.9 and 7.4  $\mu\text{g L}^{-1}$ , respectively. The analytical performance was also estimated by seedlings or immature embryos samples from three different plant tissues, pea, rice and wheat. Recoveries were in the range of 70.1–93.5%. The results show that the present imprinting method is a promising approach for preparation of selective adsorbents for sample preparation of auxin analysis in plant tissues.

© 2010 Elsevier B.V. All rights reserved.

## 1. Introduction

Auxin is one of the most crucial plant hormones in various plants, and continuously regulates the growth and development of the plants. The research of auxin has recently attracted considerable interest. Indole-3-acetic acid (IAA) is a primarily native auxin and its concentration level exquisitely controlled growing processes such

as cell elongation, division and organ formation [1–3]. The typical level of IAA in plants is in the range of 1–100  $\text{ng g}^{-1}$ , the concentration of IBA is close or lower than IAA [4]. Analysis of auxins has a great value for the study of biological process and its in-depth application, such as modern agriculture and biotechnology. However, plant hormones are difficult to analyze due to its lower concentrations in plant tissue which are very rich in interfering substances.

So far several analytical techniques have been employed for the determination of plant hormones, including HPLC [5], gas-chromatography (GC) [6], gas-chromatography mass spectrometry (GC-MS) [7], capillary electrophoresis (CE) [8] and fluorescence detection [9]. However, several isolation and enrichment processes were required because of low concentrations of plant hormones,

\* Corresponding author. Tel.: +86 20 84110922; fax: +86 20 84115107.

\*\* Corresponding author at: School of Chemistry and Chemical Engineering, Sun Yat-sen University, Xingang West Road 135, Guangzhou 510275, Guangdong, China. Tel.: +86 20 84110922; fax: +86 20 84115107.

E-mail addresses: [cesgkl@mail.sysu.edu.cn](mailto:cesgkl@mail.sysu.edu.cn), [ceshyl@mail.sysu.edu.cn](mailto:ceshyl@mail.sysu.edu.cn) (G. Li).

thus the analytical procedures were always time-consuming and solvent-depending. Thus, to utilize a solid adsorbent with specific recognition property for sample preparation would be the feasible way to solve those aforementioned problems.

Molecularly imprinted polymers (MIPs) have been widely applied in many fields of isolation [10], biosensor [11] and catalysis chemistry [12]. The imprinted technique is applied to form selective rebinding sites in a polymer matrix, exhibiting a molecular memory towards the template. The selectivity of MIPs depends on shape recognition, hydrogen bonding, and hydrophobic interactions. MIPs have been fabricated in various morphologies, such as monolith, microspheres and membrane. Recently, an extraction technique based on magnetic MIPs has received increasing attention [13–16]. The magnetic MIPs, which combine the advantages of high recognition properties of MIP and the handling convenience of magnetic separation, were obtained by encapsulating inorganic magnetic particle with organic polymer.

Synthesis of covalent MIPs for plant hormone was first implemented by Takeuchi et al. in 1998 [17]. The resultant MIPs displayed significant selectivity for the template castasterone via covalent bonding sites. However, the monomers were limited using covalent imprinted strategy. *N,N*-dimethylaminoethyl methacrylate [18,19], 2-hydroxyethyl methacrylate and 9-vinyladenine as functional monomers [20,21] were further investigated to synthesize non-covalent MIPs. This strategy was proved to be viable for imprinting of IAA, but these reported MIPs for analysis of plant hormone lacked real sample applications. The synthesis of MIPs based on non-covalent interaction has been widely used due to its simplicity and flexibility. However, the interaction between monomers and template molecule was relatively weak, especially for small template molecule. Thus, the utilization of the additive monomer in imprinted matrix can offer a multiple interaction with template molecule. This would be an alternative and efficient way to enhance the recognition capability of MIPs.

On the other hand, the main drawback of non-covalent imprinted technique is of tedious synthesis process, low available recovery, and laborious post-treatment [22]. The microwave heating initiated polymerization can offer an encouraging solution to these problems. Microwave heating was successfully used in MIPs preparation in our previous study [23], in which the reactive time can be dramatically shortened and the resultant MIPs had better morphology and recognition property. This synthetic strategy for MIPs allows the effective interaction between the template and monomer, and can potentially be employed in a routine imprinting polymerization approach.

$\beta$ -Cyclodextrin ( $\beta$ -CD) is polysaccharides of glucose with a shape of a toroid and hollow truncated cavity with the edge of the torus of the larger circumference containing chiral secondary hydroxyl groups [24]. The cavity is hydrophobic while the external face is hydrophilic. In particular, the cavity is compatible with molecules of appropriate size and shape, such as cholesterol, steroids, peptides, amino acids and drugs protein [25–30]. Furthermore,  $\beta$ -CD was widely employed as recognition reagent for rebinding guest molecules of compatible size [31,32]. Therefore, combining hydrogen bond based monomers and size-identified functional monomers would be a promising option for MIPs preparation.

In this paper, a simple and direct strategy to create magnetic MIP beads by using binary functional monomers (4-vinylpyridine and  $\beta$ -CD) as stimuli-recognition element towards IAA was reported. The polymerization was initiated by microwave heating under continuously mechanical agitation. The application and regeneration of the resulting beads were implemented by a magnetic separation process. Furthermore, an analytical method based on the mag-MIP beads with magnetic separation followed by HPLC was developed in order to determine auxins in plant tissues. The application of

the mag-MIP beads for analysis of auxins in pea, rice and wheat samples was assessed.

## 2. Experimental

### 2.1. Chemicals

IAA, indole-3-butyric acid (IBA), gibberellin A<sub>3</sub> (GA<sub>3</sub>), benzoic acid, indole, phenol, ethylene glycol (PEG 6000) and butylated hydroxytoluene (BHT) were purchased from Guanghuang Reagent Plant (Shandong, China). Azo(bis)-isobutyronitrile (AIBN) and  $\beta$ -CD were from Damao Reagent Plant (Tianjin, China). 4-Vinylpyridine (4-VP) was purchased from Sigma-Aldrich (St Louis, MO, USA). Styrene (St), trimethylolpropane trimethacrylate (TRIM), divinylbenzene (DVB), ethylene glycol dimethacrylate (EGDMA) and glycidoxypolytrimethoxysilane (GPTMS) were all obtained from Corel Chemical Plant (Shanghai, China). Methanol of HPLC grade was purchased from Merck (Darmstadt, Germany). FeCl<sub>3</sub> and FeSO<sub>4</sub> were obtained from Shenyang Chemical Reagent Plant (Shenyang, China); dimethyl formamide (DMF) and dimethylsulfoxide (DMSO) were purchased from Guangzhou Chemical Reagent Plant (Guangzhou, China). The sample eluent was filtered through a nylon 0.45  $\mu$ m filter before use.

### 2.2. Preparation and modification of Fe<sub>3</sub>O<sub>4</sub> magnetite

The Fe<sub>3</sub>O<sub>4</sub> magnetite particles were prepared using coprecipitation method [23]. Briefly, a mixture solution of 1.0 mol L<sup>-1</sup> FeCl<sub>3</sub> and 0.5 mol L<sup>-1</sup> FeSO<sub>4</sub> was homogenized and deoxygenated (nitrogen-purged). NH<sub>3</sub>·H<sub>2</sub>O (28%, w/v) was then quickly charged into the mixture at 800 rpm agitation. The resultant brown mixture was aged in microwave synthesizer from Sineo Microwave Chemistry Technology Company (Shanghai, China) at 80 °C for 1 h. The solution turned black and the precipitate was collected by a magnet and washed several times by acetic acid (10%, v/v) and distilled water. Upon completion, Fe<sub>3</sub>O<sub>4</sub> (2.0 g) and PEG (10.0 g) were mixed in water (30 mL) and then sonicated for 30 min until a homogeneous PEG–Fe<sub>3</sub>O<sub>4</sub> suspension was obtained.

### 2.3. Synthesis of magnetic MIPs beads

The derived  $\beta$ -CD was prepared according to a previous research with minor modifications [28]. 8 g of  $\beta$ -CD was dissolved in 30.0 mL dry DMF, 0.8 g NaH was added into the mixture and then stirred magnetically at 800 rpm for 1 h. This procedure presents a feasible way for deprotonation of  $\beta$ -CD. The residuary NaH was removed by filtration. Subsequently, 2.0 mL GPTMS was added dropwise into the mixture with magnetic stirring. The reaction was performed at 80 °C for 12 h. The temperature can be accurately controlled for  $\pm 0.1$  °C by an infrared temperature detector. Upon reaction completion, the solution turned thick, and the precipitation was washed with dry DMF, methanol and acetone in sequence, each time for 30 mL. The silanized  $\beta$ -CD was dried in vacuum at 110 °C for 12 h, and it was stored in a desiccator before being used.

Prior to polymerization, IAA (1.0 mmol), 4-VP (4.0 mmol) or (and) silanized  $\beta$ -CD (2.0 g) were dissolved in DMSO (10 mL) with thoroughly mixing and were then stored in dark for 12 h. The mixture, PEG–Fe<sub>3</sub>O<sub>4</sub> suspension, cross-linkers (TRIM, 23.7 mmol), monomers (St, 79.6 mmol), initiator (AIBN, 0.6 mmol) and dispersing medium (water, 80 mL) were then homogenized by agitation for 30 min to create suspension. The resulting mixture was transferred to a 300 mL single-necked flask and placed in the microwave synthesizer. The reaction mixture was continuously bubbled with a nitrogen stream to displace oxygen throughout the whole reaction process. Subsequently, the polymerization reaction was allowed to

proceed at 70 °C for 60 min. Upon completion, the resultant beads were collected by an extrinsic magnetic field. Finally, the magnetic MIP beads were extensively washed under ultrasonic with 10% acetic acid in methanol (v/v) until no leakage of IAA from the resulting beads was observed. The beads were dried under vacuum at 120 °C. Magnetic non-imprinted polymer (mag-NIP) beads were synthesized with identical conditions but with absence of template molecule.

#### 2.4. Characterization of the IAA mag-MIP beads

The morphological evaluation of IAA mag-MIP beads was examined by scanning electron microscope (SEM) from Philips (Eindhoven, Netherlands). The infrared absorption spectrum was obtained by a Shimadzu IR-prespige-21 FT-IR spectrometer (Tokyo, Japan). The thermogravimetric analysis was performed by a Netzsch STA-409 PC thermogravimetric analyzer (Bavaria, Germany). The magnetic properties analysis was measured using a SQUID-based magnetometer (San Diego, USA).

#### 2.5. Extraction procedure

Solution of IAA in methanol with different initial concentrations (0.5–500  $\mu\text{g L}^{-1}$ ) was used for the test. The beads prepared above were screened and selected in the range of 80–120  $\mu\text{m}$ . 50 mg of beads were added to a 25-mL flat-bottom vial containing 3.0 mL standard solution. The vial was incubated for extraction in a reciprocating shaking-table at 25 °C for 30 min. After extraction, the beads were magnetically separated and cleared up with 3 mL *n*-hexane to reduce non-specific adsorption. The adsorbed molecules by the polymeric beads were eluted in 1.0 mL desorption solvent. The eluent was dealt with a nitrogen drying step, and re-dissolved in 100  $\mu\text{L}$  methanol for further analysis.

#### 2.6. Competitive absorption and evaluation

A mixture standard solution of IAA, indole and benzoic acid with initial concentration of 100.0  $\mu\text{g L}^{-1}$  was incubated with mag-MIP or mag-NIP beads, and the extraction procedure was then conducted as described earlier in Section 2.5.

The interrelated absorbed coefficient was evaluated by the following equations:

$$\text{static distribution coefficient : } K_d = \frac{C_p}{C_s}$$

where  $C_p$  is the concentration on the absorbed medium and  $C_s$  is the final free concentrations of the solution. For comparison of the obtained mag-MIP beads selectivity, the selectivity coefficient  $k$  and relative selectivity coefficient  $k'$  values were calculated as the following formula:

$$\text{selectivity coefficient : } k = \frac{K_{d(\text{IAA})}}{K_{d(\text{Referent})}}$$

where  $K_{d(\text{IAA})}$  and  $K_{d(\text{Referent})}$  are the static distribution coefficients of template and referent molecules, respectively.

$$\text{relative selectivity coefficient : } k' = \frac{k_{\text{MIP}}}{k_{\text{NIP}}}$$

where  $k_{\text{MIP}}$  and  $k_{\text{NIP}}$  represent selectivity coefficient of mag-MIP beads and mag-NIP beads, respectively.

#### 2.7. Chromatographic conditions

The chromatographic analysis was performed by using a Shimadzu LC-2010 unit with a UV-vis detector and a reversed phase

$\text{C}_{18}$  column from Dikma (Beijing, China). The mobile phase consisted of 0.45% acetic acid (v/v) in water and methanol. The linear gradient elution was performed with methanol increasing from 25 to 75% (v/v) in 30 min, and the flow rate was set at 1.0  $\text{mL min}^{-1}$ . The detection wavelength was 260 nm.

#### 2.8. Sample analysis

The seedlings and immature embryos of pea, rice and wheat were selected for the spiked sample analysis. After collecting 100 g 3–4 cm average-high of seedling or immature embryos, the samples were homogenized in 50 mL methanol with 0.1% BHT (w/v) to prevent IAA and IBA from oxidation. The spiked samples were prepared by mixing standard solutions of IAA and IBA (initial concentration of 1.0  $\text{mg L}^{-1}$ ) with the homogenized sample. Then the samples were incubated at –20 °C for 12 h in darkness. Afterwards, the homogenates were filtered through a 0.45  $\mu\text{m}$  nylon filter, and then the residue was rinsed thrice by 50 mL cold methanol. The extract was collected and distilled at 45 °C under reduced pressure. The concentrated extract was purified three times by equivalent volume of petroleum ether, and then was extracted three times with *n*-hexane (after adjusted pH value of the aqueous solution at 3.0 with 0.10  $\text{mol L}^{-1}$  hydrochloric acid). The organic phases (~10 mL each) were collected and subjected to the extraction procedure by mag-MIP beads. The spiked concentrations were obtained at three levels of 10.0, 40.0 and 80.0  $\mu\text{g kg}^{-1}$  for IAA and IBA. Eventually, the extract was determined under the optimized experimental conditions by the developed methods. The reproducibility (between-assay precision) was based on three separate runs.

### 3. Results and discussion

#### 3.1. Preparation of mag-MIP beads by microwave heating-induced polymerization

The synthesis of magnetic micron-size beads by microwave heating has been originally reported in our previous study [23]. In this paper, microwave heating was also applied as the extraneous energy for synthesis of IAA imprinted magnetic beads with some modification. The preparation protocol is described in Fig. 1. The approach included the following procedure: (1) obtaining the magnetic cores with surface modification by PEG; (2) derivatization of  $\beta$ -CD; (3) self-assembly of the template and functional monomers; (4) polymerization of the polymeric mixture initiated by microwave heating in the presence of crosslinker, initiator and dispersing medium. Recognition cavities of the resulting beads were achieved by eluting template molecules.

Initially,  $\text{Fe}_3\text{O}_4$  particles were produced using coprecipitation, followed by aging with microwave heating at 80 °C for 1 h. The average diameter of the  $\text{Fe}_3\text{O}_4$  particles, measured by transmission electron microscope, was obtained at the range from 15 to 20 nm. For bare magnetite, it is difficult to uniformly encapsulate polymer beads by physical embedding, which has been demonstrated in previous studies for biomacromolecular immobilization [33]. Therefore, the  $\text{Fe}_3\text{O}_4$  magnetite which was prepared by coprecipitation method has been modified for further encapsulation. In this work, the magnetite was coated with PEG, which introduced polymeric chain on the surface of the magnetite. As a result, the capsulation of the magnetite in suspended droplets can be improved.

The monomer was the most important factor for generating the recognition sites through organized self-assembly with the template IAA, and was discussed in detail concerning the extraction ability and selectivity in the next section. The cross-linker

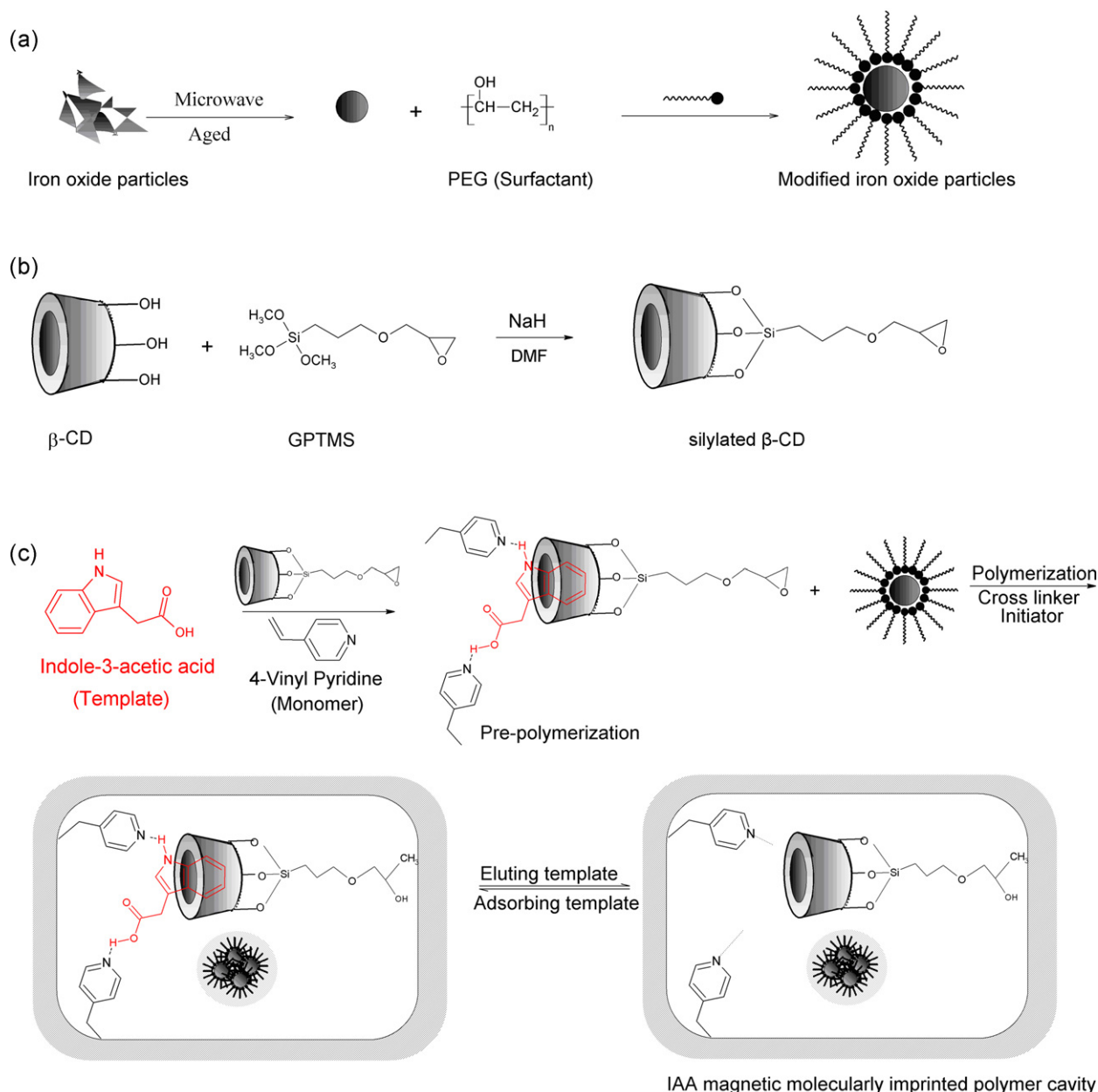


Fig. 1. Schematic representation of PEG modification of iron oxide particles (a), the silanization of  $\beta$ -CD (b) and IAA mag-MIP beads preparation (c).

was investigated using an equivalent molar amount ( $\sim 24$  mmol) of TRIM, DVB and EGDMA. The experimental results indicated that the beads prepared with TRIM provided the right balance of flexibility and rigidity, and better uniform spherical shape than either EGDMA or DVB did. It is crucially important for the subsequent application and regeneration of resulting beads.

The morphological structure and recognition capability of the MIPs were influenced markedly by the polymerization solvent. Usually, polymerization in the low-polar solvent was benefit for production of recognition sites. It was investigated by using toluene, acetone, ethanol, tetrahydrofuran (THF) and DMSO as prepolymerization solvent via observing reaction status and the morphology of the resultant beads. IAA was undissolved in toluene. Less MIPs with spherical shape were produced when acetone, THF or ethanol were used as solvent, respectively. Eventually, the beads were successfully prepared with DMSO as prepolymerization solvent, and good homogeneity and density of the resultant beads could be reproduced.

The approach of microwave heating for the imprinted polymerization has been studied in our previous work [23]. In this work, the microwave heating time was further optimized in the range of 30–120 min. From batch rebinding experiments results, the beads prepared by microwave heating for 60 min showed the highest binding amounts, and longer heating time did not show noticeable increase in rebinding capability of the resultant beads. Therefore, 60 min of microwave heating was chosen for IAA mag-MIPs beads preparation.

### 3.2. Binding capability using different functional monomers

The comparison of the binding capability of mag-MIP and mag-NIP beads prepared from different monomers was studied by the simultaneous analysis of IAA and IBA standard solution. In this work, AA, MAA, 4-VP and  $\beta$ -CD as functional monomers were studied. In order to improve the compatibility of  $\beta$ -CD, GPTMS was used to modify  $\beta$ -CD through the chemical bonding, as shown in

**Table 1**  
Comparison of the imprinting efficiency with different functional monomers.

Functional monomers	Extracted yields (pmol)	Imprinting capacity (%)	Imprinting efficiency <sup>a</sup>
$\beta$ -CD/4-VP (MIP)	210	40.9	2.23
$\beta$ -CD/4-VP (NIP)	94.0	18.3	
4-VP (MIP)	135	26.3	1.47
4-VP (NIP)	92.0	17.9	
$\beta$ -CD (MIP)	118	23.0	1.36
$\beta$ -CD (NIP)	87.0	16.9	

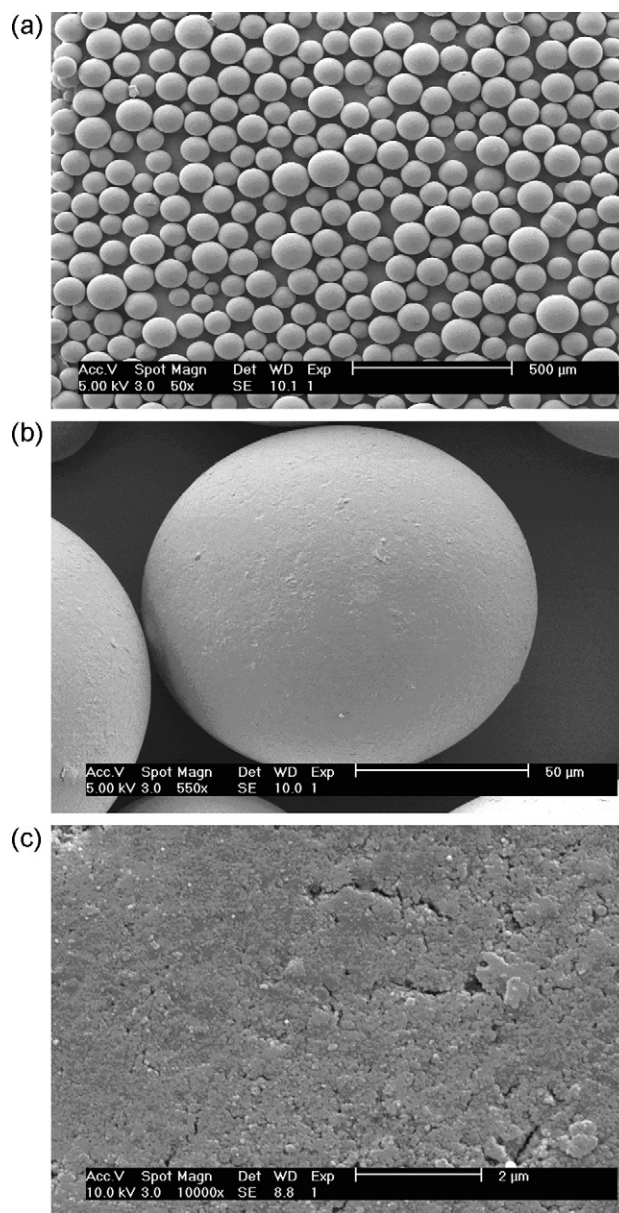
<sup>a</sup> The imprinting capacity was calculated from the extracted yields ( $Q$ ) and the initial amounts of the compounds ( $B$ ) (imprinting capacity =  $100\% \times Q/B$ ), and imprinting efficiency was calculated from extraction yield of mag-MIP ( $Q_{MIP}$ ) and that of mag-NIP ( $Q_{NIP}$ ) beads (imprinting efficiency =  $Q_{MIP}/Q_{NIP}$ ).

Fig. 1b. AA, MAA, 4-VP and  $\beta$ -CD have been individually applied as the monomer to compare the imprinting efficiency, which were obtained by the ratio of the target molecules bound to the mag-MIP to those bound to mag-NIP beads. Results showed the utilization of 4-VP gave the highest binding amounts for IAA. Moreover, the addition of  $\beta$ -CD in the 4-VP imprinted system had showed a dramatic enhancement of rebinding capacity for IAA and IBA (Supplementary Material Fig. S1). The mechanism that influence the recognition capability would be ascribed to multiple affinity, including the complementary of  $\beta$ -CD cavity and the indole ring of IAA, as well as hydrogen bond interaction between the amino of 4-VP and carboxyl group of IAA. The analytical results are illustrated in Table 1. The imprinting efficiency of the mag-MIP beads prepared by adopting 4-VP and  $\beta$ -CD in combination as binary monomer was obtained at 2.23, which was higher than 1.47 and 1.36 for the mag-MIP prepared by using the monomer 4-VP or  $\beta$ -CD separately. In this sense, improvement of imprinting efficiency was possibly ascribed to the application of the multiple monomers in the resultant imprinted beads. When template, such as IAA, is small and possess less functional groups, the interaction with single monomer was fragile. The binary monomers were allowed to self-assemble with the template IAA through inclusion, hydrogen interaction, hydrophobic interaction, as well as shape recognition. Therefore, the adsorption results revealed that the use of  $\beta$ -CD as additive functional monomer could offer a better molecular recognition in imprinted system. The role of  $\beta$ -CD as functional monomer for improvement of molecular recognition was also reported in other Ref. [28].

### 3.3. Characteristics of the IAA mag-MIP beads

The resulting beads were employed to study the morphology feature by scanning electron microscope (SEM). From the images in Fig. 2, it can be seen that uniform and spherical shape of the mag-MIP beads were obtained. Moreover, a porous and rough surface was observed, this resulted in a high specific surface area and rapid equilibrium for the adsorption and desorption kinetics. The diameter distribution of the beads was from 50 to 200  $\mu$ m, and the majority (80%) was from 80 to 150  $\mu$ m which was measured by particle size analysis (Supplementary Material Fig. S2)

FT-IR spectra (Supplementary Material Fig. S3) were used to monitor the polymerization reaction. The spectra of the resulting beads showed corresponding infrared absorption peaks to the main functional groups. A distinct absorption band including 537 and 538  $\text{cm}^{-1}$  was attributed to Fe–O bond from  $\text{Fe}_3\text{O}_4$  particles. A broad absorption band at 3410  $\text{cm}^{-1}$  was corresponded to the stretching vibration of O–H bonds of the hydroxyl groups of  $\beta$ -CD (monomer). The typical bands of the beads at 1600  $\text{cm}^{-1}$  were due to 4-VP (monomer), 3030 and 2930  $\text{cm}^{-1}$  due to the C–H aromatic stretching vibrations of styrene units. Other absorption bands, such as 1730  $\text{cm}^{-1}$  (stretching vibration of C=O bonds of carbonyl groups) and 1450  $\text{cm}^{-1}$  (stretching vibration of C=H



**Fig. 2.** Scanning electron micrographs of IAA mag-MIP beads prepared by microwave heating. Magnifications: (a): 50 $\times$ , (b): 550 $\times$ , (c): 1  $\times$  10<sup>4</sup> $\times$ .

bonds of phenyl) matched both for magnetic mag-MIP and mag-NIP beads.

The magnetization curve of the resulting beads was measured by magnetic hysteresis loops analysis, in which no hysteresis, remanence and coercivity were observed. The saturation magnetization was 1.12 emu/g for the mag-MIP beads and 1.03 emu/g for the mag-NIP beads, respectively (Supplementary Material Fig. S4). It meant that the resulting beads can be rapidly attracted or released by an external magnetic field.

The magnetite content was further evaluated by thermogravimetric analysis (Supplementary Material Fig. S5). Scarce mass loss occurred under the temperature of 310  $^{\circ}\text{C}$ , and then degradation was observed with  $\sim$ 90% weight-loss from 310  $^{\circ}\text{C}$  to 580  $^{\circ}\text{C}$ . The remaining mass heating up to 800  $^{\circ}\text{C}$  was attributed to magnetite particles with thermal resistance. It was concluded that the magnetite content was 0.48% for mag-MIP and 0.43% for mag-NIP beads, respectively. Solvent resistant analysis for the resulting beads was tested by several different solvents, possibly adopted in

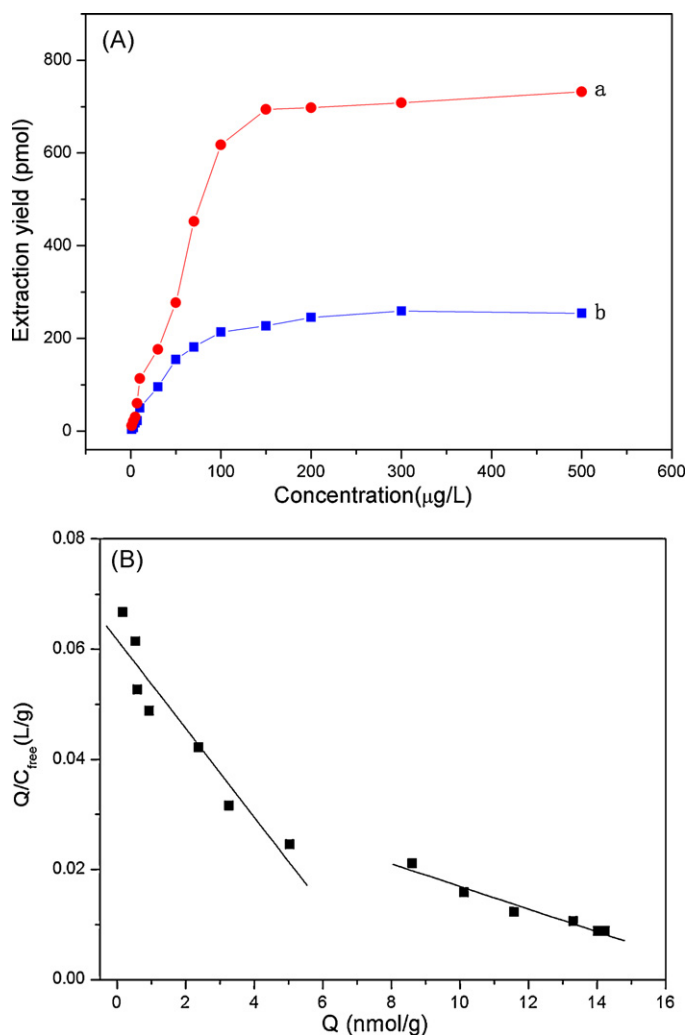


**Fig. 3.** (A) Extraction amount curves of IAA mag-MIP (a) and mag-NIP beads (b) to IAA standard solutions of 0.500–500.0 μg L<sup>-1</sup>. (B) Scatchard plot of mag-MIP beads for IAA.

this method. The resulting beads were incubated in solvents like methanol, acetonitrile, 10% acetic acid in methanol (v/v) and 10% acetic acid in acetonitrile (v/v) in ultrasonic bath, each time for 1 h. A good surface quality and no desquamating or cracking of the resulting beads were found in these solvents, indicating that the mag-MIP beads could be suitable for the subsequent application coupled with HPLC analysis. Furthermore, the longevity of the magnetic MIP beads was investigated. It was proved that the beads can be reused at least 100 times.

From the above characteristic evaluation of mag-MIP and mag-NIP beads, there is no significant difference between mag-MIP and mag-NIP beads. The following study had proved that the different binding capabilities would attribute to the molecular imprinting effect rather than morphological differences.

### 3.4. Adsorption properties of the IAA mag-MIP beads

#### 3.4.1. Batch rebinding investigation

A series of IAA standard solutions with concentrations of 0.100–500.0 μg L<sup>-1</sup> were used to evaluate the rebinding capability of the mag-MIP and mag-NIP beads (Fig. 3(A)). It can be seen that the extraction amounts increased with increasing concentrations in the range of 0.500–200.00 μg L<sup>-1</sup> for mag-MIP beads, and the equilibrium was achieved as the concentration was up to 200.00 μg L<sup>-1</sup>.

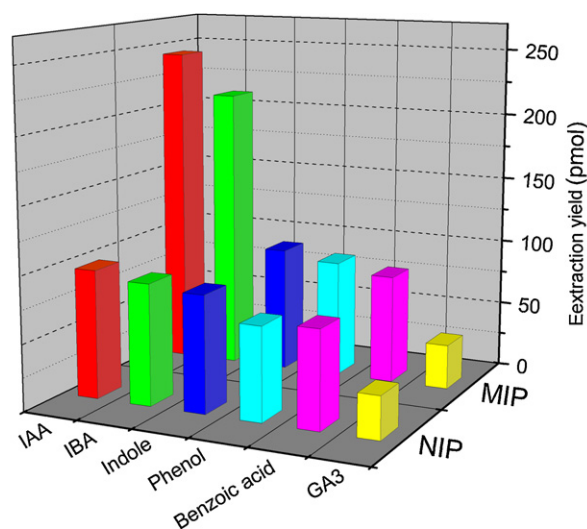
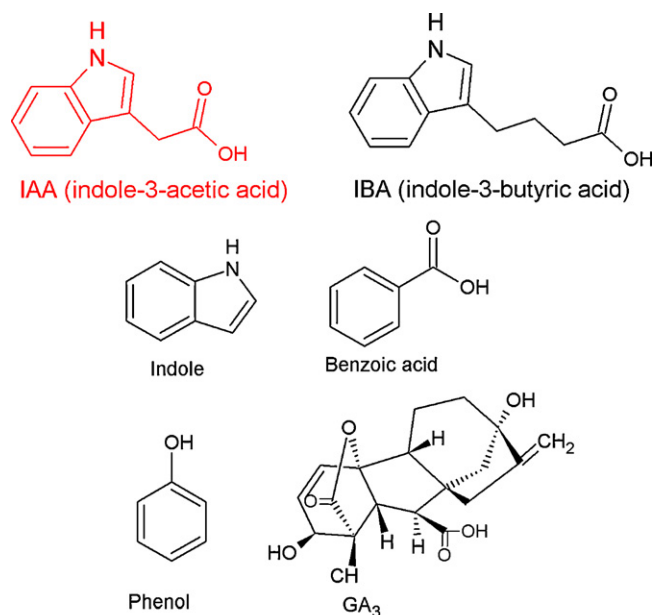


**Fig. 4.** Extraction yields of indole-3-acetic acid, its structural analogues (indole-3-butyric acid, IBA) and reference compounds (indole, benzoic acid, phenol and gibberellins) extracted with IAA mag-MIP and mag-NIP beads at 30.00 μg L<sup>-1</sup> level.

The total adsorption capacity was 780 pmol for IAA. On the other hand, the adsorption capacity of mag-NIP beads was only 200 pmol, which was attributed to non-imprinted efficiency existed in polymer matrix.

In order to further study the binding properties of the mag-MIP beads, Scatchard analysis was performed. The calculated equation was exhibited as following:

$$\frac{Q}{C_{\text{free}}} = \frac{Q}{K_D} + \frac{Q_{\text{max}}}{K_D}$$

where  $Q$  is the amount of IAA bound to mag-MIP beads at equilibrium,  $C_{\text{free}}$  is the free IAA concentration in matrix solution,  $Q_{\text{max}}$  is the maximum binding capacity, and  $K_D$  is the dissociation constant. It is possible to estimate the  $Q_{\text{max}}$  and  $K_D$  from this plot. As shown in Fig. 3(B), the binding sites of the plot were favorably linearized into two segments. It is suggested that there is probably higher affinity site and lower affinity site with MIPs. According to the linear regression formulas, the binding constants of  $Q_{\text{max}1} = 7.6 \text{ L g}^{-1}$  and  $K_{D1} = 123.9 \text{ nmol g}^{-1}$  for higher affinity site and  $Q_{\text{max}2} = 18.4 \text{ L g}^{-1}$

**Table 2**  
The selectivity parameters of the mag-MIP and mag-NIP beads.

Samples	$C_p$ ( $\mu\text{g/g}$ )			$C_s$ ( $\mu\text{g L}^{-1}$ )			$K_d$ ( $\text{mL/g}$ )			$k^a$		$k'^a$	
	IAA	Indole	Benzoic acid	IAA	Indole	Benzoic acid	$K_{d1}$ (IAA)	$K_{d2}$ (Indole)	$K_{d3}$ (Benzoic acid)	$k_1$	$k_2$	$k'_1$	$k'_2$
MIP	2.711	0.661	0.482	0.055	0.089	0.092	49.29	7.427	5.239	6.64	9.41	5.78	3.65
NIP	0.816	0.723	0.363	0.086	0.088	0.094	9.488	8.215	3.682	1.15	2.58		

<sup>a</sup>  $k$ , selectivity coefficient:  $k_1 = K_{d1}/K_{d2}$ ,  $k_2 = K_{d1}/K_{d3}$ ;  $k'$ , relative selectivity coefficient:  $k' = k_{\text{MIP}}/k_{\text{NIP}}$ ,  $k'_1 = k_{1\text{MIP}}/k_{1\text{NIP}}$ ,  $k'_2 = k_{2\text{MIP}}/k_{2\text{NIP}}$ .

and  $K_{D2} = 471.4 \text{ nmol g}^{-1}$  for lower affinity site could be obtained.

### 3.4.2. Adsorption and desorption kinetics

Kinetic study of the adsorption and desorption was carried out for both mag-MIP and mag-NIP beads as described in the above rebinding test with initial IAA concentration of  $30.00 \mu\text{g L}^{-1}$  (Supplementary Material Fig. S6). Both the mag-MIP and mag-NIP reached equilibrium in the first 30 min. At similar test conditions, fast desorption rates were also observed for both mag-MIP and mag-NIP beads. Most IAA bound on the beads could be easily eluted within 10 min. The rapid kinetic process authentically estimated the advantages of imprinting approach and the special morphology of the resulting beads.

### 3.4.3. Adsorption selectivity

The selectivity of the mag-MIP and mag-NIP beads was investigated by measuring extraction amounts of IAA, IBA and reference molecule with mixed standard solution at  $30.00 \mu\text{g L}^{-1}$  level. The results of the study are shown in Fig. 4. For mag-MIP beads, the IAA and IBA loadings were obtained at 240 and 201 pmol, while much lower IAA loading of 98 pmol and IBA of 87 pmol was observed for mag-NIP beads. This high selectivity mainly owns to the molecular size recognition and the hydrogen bonding between polymeric matrix and template. On the other hand, the adsorption of mag-MIP beads for the reference molecules (indole, phenol, benzoic acid, and  $\text{GA}_3$ ) was not obviously different to those of mag-NIP beads, and the amounts are below 80 pmol level. This showed that, in the case of reference molecules, the adsorption was likely depended on the mechanism of non-specific interaction. In order to further investigate the molecular recognition property imparted to the mag-MIP, indole and benzoic acid as reference molecules with  $100.0 \mu\text{g L}^{-1}$  of initial concentration were chosen to measure the selectivity parameters. The values of  $K_d$ ,  $k$  and  $k'$  are calculated in Table 2. The static distribution coefficient ( $K_d$ ) is defined as the ratio of the concentrations of the solute at the two phases under equilibrium state, and is calculated to be  $49.29 \text{ mL g}^{-1}$  of IAA for mag-MIP beads

and  $9.488 \text{ mL g}^{-1}$  for mag-NIP beads. The selectivity coefficient ( $k$ ) indicated the cross-selectivity between the reference compound and the target molecule. It can be seen from Table 2 that significantly high  $k$  value of 6.64 and 9.41 of mag-MIP beads had been achieved, which indicated high discrimination property of the mag-MIP beads between the template and other compounds.

## 3.5. Application of the magnetic MIP beads to analysis of auxins in plant tissue

### 3.5.1. Analytical performances

After optimization of the extraction conditions, such as extraction solvent, extraction time and desorption time, the linearity was evaluated with different concentrations of IAA and IBA mixed standard solutions ( $0.050$ – $300.00 \mu\text{g L}^{-1}$ ). The linear range of the mag-MIP beads extraction coupled with HPLC method was established to be  $7.00$ – $100.00 \mu\text{g L}^{-1}$  for IAA and  $10.00$ – $100.00 \mu\text{g L}^{-1}$  for IBA. The correlation coefficient of the calibration graphs is 0.9969 for IAA and 0.9911 for the IBA. For calculation of the detection limits (LOD), we used three times standard deviations of calibration curves divided by their slopes. The LOD of IAA and IBA were 3.9 and  $7.4 \mu\text{g L}^{-1}$ , respectively. The precision of the method was investigated with  $30.00 \mu\text{g L}^{-1}$  mixed standard solution of IAA and IBA, and the relative standard deviations (RSDs) varied from 6.8 to 8.3% ( $n = 6$ ).

### 3.5.2. Real sample analysis

The different plant tissues were used to examine the feasibility of the mag-MIP beads on real sample applications, and the results were compared with the mag-NIP beads. Endogenous auxin content in seedlings and immature embryos in pea, rice and wheat were measured. These samples were also selected for spiked analysis for validation of the method. The spiking concentrations for each auxins at three levels of 10.0, 40.0, and  $80.0 \mu\text{g kg}^{-1}$ , were subjected to extraction by the mag-MIP beads and then analyzed by HPLC. Fig. 5 shows the chromatogram of the rice sample as an example to express the selectivity of the mag-MIP beads. The results revealed

**Table 3**  
Recoveries ( $R$ ) of auxins for spiked samples ( $n = 3$ ).

Sample	Compound	Endogenous content ( $\mu\text{g kg}^{-1}$ )	$10.0 \mu\text{g kg}^{-1}$		$40.0 \mu\text{g kg}^{-1}$		$80.0 \mu\text{g kg}^{-1}$	
			$R$ (%)	RSD (%)	$R$ (%)	RSD (%)	$R$ (%)	RSD (%)
Pea embryo	IAA	7.5	73.6	10.9	77.5	9.5	78.6	11.5
	IBA	–	70.1	13.9	73.3	13.2	77.8	10.1
Rice embryo	IAA	15.1	82.3	10.3	80.5	9.2	81.4	9.9
	IBA	–	78.8	9.8	89.3	8.8	88.0	9.1
Wheat embryo	IAA	13.7	78.0	12.1	82.8	11.5	82.9	9.3
	IBA	–	85.4	10.0	93.5	8.7	92.6	8.5
Pea seedling	IAA	10.8	81.7	8.2	88.7	10.1	87.5	8.1
	IBA	–	79.8	9.5	85.1	8.5	82.2	7.9
Rice seedling	IAA	16.0	83.5	8.9	86.5	9.1	87.9	8.8
	IBA	–	85.4	11.0	83.5	9.4	82.6	7.4
Wheat seedling	IAA	19.3	82.4	10.3	75.6	7.9	90.8	8.0
	IBA	–	82.3	9.7	89.7	8.1	89.0	9.7

“–”: Could not be detected.

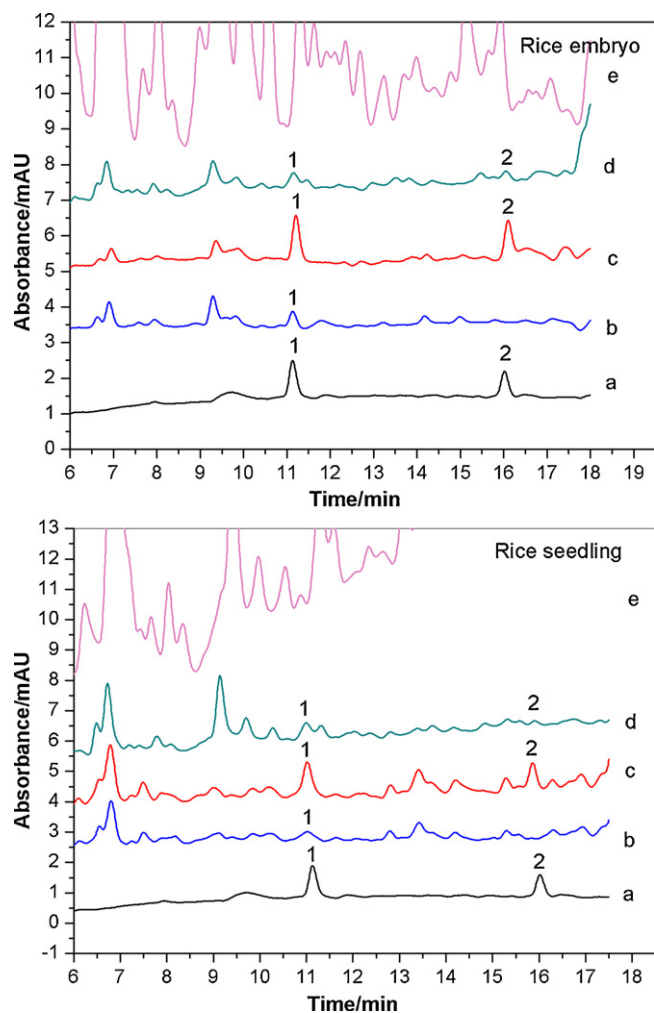


**Fig. 5.** Chromatograms of rice seedling and rice embryo samples. (a) 1.00 mg L<sup>-1</sup> mixed auxins standard solution; (b) samples extracted with the mag-MIP beads; (c) 40.00  $\mu\text{g kg}^{-1}$  auxins spiked samples extracted with mag-MIP; (d) 40.00  $\mu\text{g kg}^{-1}$  auxins spiked samples extracted with mag-NIP beads; (e) Raw solutions of samples; peaks: 1, IAA; 2, indole-3-butyric acid, injection volume of 20  $\mu\text{L}$ .

that the chromatogram was very complex by direct injection of raw solution, but was significantly cleaner after extraction by the mag-MIP beads. It was mainly due to the recognition of the formed cavities in MIP network. However, auxins could not be well quantified by extraction with the mag-NIP beads. The recoveries of the spiked embryos and seedlings in pea, rice and wheat samples were from 70.1% to 93.5%, and the RSDs were from 7.4% to 13.9%, respectively. The endogenous IAA in the embryos of pea, wheat and rice were 7.5, 15.1 and 13.7  $\mu\text{g kg}^{-1}$ , and in the seedling were 10.8, 16.0 and 19.3  $\mu\text{g kg}^{-1}$  respectively, meanwhile IBA was totally not accurately quantified (Table 3). It could be seen that a reliable analytical method based on the mag-MIP beads extraction coupled with HPLC allowed the highly selective detection of auxins at trace levels in complicated matrix by the proposed method.

#### 4. Conclusions

A novel method for the highly selective recognition of auxins was developed based on molecularly imprinting technique and magnetic separation. The IAA mag-MIP beads were prepared by using microwave heating initiated polymerization. Several artificial magnetic receptors for IAA were synthesized with solo or binary functional monomers, respectively. Their binding capability for

auxins was further evaluated. A higher rebinding capacity for template was obtained by the mag-MIP beads imprinted with binary monomers composed of 4-VP and  $\beta\text{-CD}$ . The IAA mag-MIP beads were then applied to auxin analysis from seedlings and immature embryos in three different plant tissues, pea, rice and wheat. The analytical results of plant samples display that the present imprinting method is a promising approach for obtaining highly selective adsorbent for sample preparation of auxins in plant tissues. It is further envisaged that the feasibility of preparing mag-MIP beads by using microwave heating and multiple functional monomers could provide a promising alternative for rapid synthesis of MIP with improved recognition capability.

#### Acknowledgements

The authors would like to thank the National Natural Science Foundation of China for financially supporting this research under grant numbers 90817012, 20775095, 20705042, and 21075140, the Key Program of Guangdong Provincial Natural Science Foundation of China under grant number of 9251027501000004, and the Fundamental Research Funds for the Central Universities, respectively.

#### Appendix A. Supplementary data

Supplementary data associated with this article can be found, in the online version, at doi:10.1016/j.chroma.2010.09.059.

#### References

- [1] A.W. Woodward, B. Bartel, *Ann. Bot.* 95 (2005) 707.
- [2] E. Epstein, J. Ludwig-Müller, *Physiol. Plant* 88 (1993) 382.
- [3] J. Rivov, S.F. Yang, *Plant Growth Regul.* 8 (1989) 131.
- [4] M.L. Brenner, *Annu. Rev. Plant Physiol.* 32 (1981) 511.
- [5] B. Monlero, J. Sibole, C. Cabot, C. Poschenrieter, J. Barcelo, *J. Chromatogr. A* 658 (1994) 83.
- [6] B. Vermeer, B. Knecht, J. Bruinsma, *J. Chromatogr.* 404 (1987) 346.
- [7] W.J. Hunter, *J. Chromatogr.* 362 (1986) 430.
- [8] B.F. Liu, X.H. Zhong, Y.T. Lu, *J. Chromatogr. A* 945 (2002) 257.
- [9] J. Olsson, K. Claeson, B. Karlberg, *J. Chromatogr. A* 824 (1998) 231.
- [10] J. O'Mahony, A. Molinelli, K. Nolan, M.R. Smyth, B. Mizaikoff, *Biosens. Bioelectron.* 21 (2006) 1383.
- [11] A. Ersöz, S.E.A. Dilemiza, A.A. Özcan, A. Denizli, R. Say, *Biosens. Bioelectron.* 24 (2008) 742.
- [12] A. Visnjeviski, R. Schomäcker, E. Yilmaz, O. Brüggemann, *Catal. Commun.* 6 (2005) 601.
- [13] J.A. Richard, M. Klaus, *Analyst* 121 (1998) 611.
- [14] L.G. Chen, X.P. Zhang, Y. Xu, X.B. Du, X. Sun, L. Sun, H. Wang, Q. Zha, A.M. Yu, H.Q. Zhang, L. Ding, *Anal. Chim. Acta* 662 (2010) 31.
- [15] L.G. Chen, J. Liu, Q.L. Zeng, H. Wang, A.M. Yu, H.Q. Zhang, L. Ding, *J. Chromatogr. A* 1216 (2009) 3710.
- [16] Y.S. Ji, J.J. Yin, Z.G. Xu, C.D. Zhao, H.Y. Huang, H.X. Zhang, *Anal. Bioanal. Chem.* 395 (2009) 1125.
- [17] A. Kugimiya, J. Matsui, H. Abe, M. Aburatani, T. Takeuchi, *Anal. Chim. Acta* 365 (1998) 75.
- [18] A. Kugimiya, T. Takeuchi, *Anal. Chim. Acta* 395 (1999) 251.
- [19] A. Kugimiya, T. Takeuchi, *Electroanalysis* 11 (1999) 1158.
- [20] A. Kugimiya, T. Takeuchi, *Anal. Bioanal. Chem.* 372 (2002) 305.
- [21] Ch. Chen, Y. Chen, J. Zhou, C. Wu, *Anal. Chim. Acta* 569 (2006) 58.
- [22] K. Haupt, *Anal. Chem.* 75 (2003) 376A.
- [23] Y. Zhang, R.J. Liu, Y.L. Hu, G.K. Li, *Anal. Chem.* 81 (2009) 967.
- [24] E. Schneiderman, A.M. Stalcup, *J. Chromatogr. B* 745 (2000) 83.
- [25] Y. Egawa, Y. Shimura, Y. Nowatari, D. Aiba, K. Juni, *Int. J. Pharm.* 293 (2005) 165.
- [26] H. Takayuki, K. Masaya, A. Hiroyuki, K. Makoto, S. Masahiko, K. Masaya, *Macromolecules* 32 (1999) 2265.
- [27] S.H. Song, K. Shirasaka, M. Katayama, S. Nagaoka, T. Yoshihara, J. Osawa, H. Sumaoka, H. Asanuma, M. Komiyama, *Macromolecules* 40 (2007) 3530.
- [28] L. Qin, X.W. He, W.Y. Li, Y.K. Zhang, *J. Chromatogr. A* 1187 (2008) 94.
- [29] S.M. Ng, R. Narayanaswamy, *Sens. Actuators B* 139 (2009) 156.
- [30] W. Zhang, L. Qin, X.W. He, W.Y. Li, Y.K. Zhang, *J. Chromatogr. A* 1216 (2009) 4560.
- [31] H. Asanuma, T. Akiyama, K. Kajiji, T. Hishiya, M. Komiyama, *Anal. Chim. Acta* 435 (2001) 25.
- [32] G. Ermondi, C. Anghilante, G. Caron, *J. Mol. Graphics Model.* 25 (2006) 296.
- [33] M. Suzuki, M. Shinkai, M. Kamihira, T. Kobayashi, *Biotechnol. Appl. Biochem.* 21 (1995) 335.